RESEARCH PAPER

Acta Neurobiol Exp 2020, 80: 375–380
DOI: 10.21307/ane-2020-034

A smaller olfactory bulb in a mouse model of Down syndrome

Pietro Bontempi[1#], Barbara Cisterna[2#], Manuela Malatesta[2], Elena Nicolato[2,3], Carla Mucignat-Caretta[4*] and Carlo Zancanaro[2]

[1] Department of Computer Science, University of Verona, Verona, Italy,
[2] Department of Neurosciences Biomedicine and Movement Sciences, University of Verona, Verona, Italy,
[3] Centro Piattaforme Tecnologiche dell'Università di Verona,Verona, Italy,
[4] Department of Molecular Medicine, University of Padova, Padova, Italy,
[#] These two authors contributed equally to this work,
[*] Email: carla.mucignat@unipd.it

Persons with trisomy 21 (Down syndrome) present different phenotypes, including early neurodegeneration, which is prominent in the brain olfactory areas, and olfactory deficit. The use of in vivo techniques in animal models allows to characterize and follow up these slowly developing phenomena. We explored by means of magnetic resonance imaging the olfactory bulb of the Ts65Dn mouse, an established model of Down syndrome, searching for possible syndrome-related changes. In vivo imaging provided a first glimpse of the trisomic olfactory bulb as compared to euploid one. The olfactory bulb volume was smaller in trisomic mice, suggesting that changes in olfactory bulb may be apparent already in the young adult (2- to 8-month-old) mice, which are amenable to follow-up *in vivo*. These findings lead the way to future work aimed at characterizing the Down syndrome-related development of morphological alterations in the olfactory bulb and relating them to changes in olfactory performance, which were detected in this mouse model.

Key words: *in vi*vo imaging, olfaction, trisomy, olfactory bulb, Down syndrome

INTRODUCTION

Down syndrome (DS), which affects approximately 1 out of 700 live births (Parker et al., 2010) is characterized by trisomy of chromosome 21. DS is characterized by several conditions including intellectual disability, craniofacial alterations, congenital heart disease, early onset Alzheimer's disease, gastrointestinal disorders, low muscle strength (Korenberg et al., 1994). Olfactory dysfunction has been consistently found in DS (Murphy et al., 1996; Cecchini et al., 2016) together with age-associated development of Alzheimer's disease neuropathology in the olfactory system, starting from the entorhinal and trans-entorhinal areas (Price et al., 1991), as well as neurodegenerative pathology (Mann et al., 1986). The olfactory bulb (OB) is the first central relay station of the peripheral olfactory neurons playing a key role in olfactory processing (Mori et al., 1999). In the OB, multiple types of neurons network to process information and transmit it to the olfactory cortex. Despite several techniques have been used to investigate the DS brain in vivo (review in Neale et al., 2017), information on OB status in living persons with DS is quite limited.

The Ts65Dn mouse is one of the most extensively studied animal models of DS. It presents segmental trisomy for chromosome 16 and involves roughly half of human chromosome 21 orthologs (Davisson et al., 1993). In the Ts65Dn mouse, smell impairments appear in adulthood (Bianchi et al., 2014) since reduced neuro-

Received 6 April 2020, accepted 6 July 2020

genesis takes place: this has been suggested to underlie hypocellularity of the OB, ultimately leading to deficit in olfactory learning through a reduction in the number of new granule neurons migrating to the OB from the subventricular zone. This has been challenged by others (López-Hidalgo et al., 2016). Similar alterations have also been observed in persons with DS. Moreover, Ts65Dn mice present impaired refinement of synaptic connections by olfactory neurons in the OB (William et al., 2017). Accordingly, investigating the OB in the Ts65Dn mouse is relevant to clarify the mechanisms of olfactory impairment in DS. Magnetic resonance imaging (MRI) is a recognized, powerful and non-invasive tool to investigate the *in vivo* morphology and function of organs in both humans and experimental animals. Using the same technology, MRI findings in experimental animals can be easily translated to the patient. In this work we examined trisomic and euploid Ts65Dn mice by means of MRI to highlight possible DS-related changes in the OB. In particular, we focused on an MRI protocol that could provide structural and anatomical insight in the DS-related changes of the OB, while being compatible with *in vivo* examination in a fragile animal model.

METHODS

Ts65Dn (strain: B6EiC3Sn.BLia-Ts(17<16>)65Dn/DnJ) breeder mice were obtained from the Jackson Laboratory, ME, USA. The colony was maintained by breeding trisomic female mice to euploid B6EiC3Sn.BLiAF1/J males. Pups were weaned at 21 days of age. Tissue for genotyping was obtained from tail clips in p11 mice. Genotyping was accomplished by Mmu17 translocation breakpoint separated PCR. Adult (2-8 months of age) male Ts65Dn mice (8 trisomic and 8 euploid) were used in this work. Male mice were chosen for this study because of lack of variability associated with the estrous cycle. Mice were housed in groups of 3-4 by genotype and maintained under standard conditions (24±1°C temperature, 60±15% relative humidity, and 12 h light/dark cycle) and fed *ad libitum* with standard commercial chow.

The experimental protocol was reviewed and authorized according to EU Directive 2010/63/EU by the Italian Ministry of Health (ref.: 538/2015-PR).

For MRI, mice were anesthetized by inhalation of a mixture of air and O_2 containing 0.5–1% isoflurane and placed prone with their head in stereotactic position.

Images were acquired using a Biospec Tomograph (Bruker, Karlsruhe, Germany) equipped with a 4.7 T, 33 cm bore horizontal magnet (Oxford Ltd, Oxford, UK). A double coil configuration was used: the excitation r.f. pulses were applied trough a 7.2 cm bird cage volume coil, while the signal was received through a 2-channel surface coil optimized for the mouse brain (Bruker). After a sagittal scout image, 6-7 contiguous 0.5 mm-thick slices were acquired through the whole OB using a RARE T_2-weighed sequence with TR (repetition time) = 5000 ms, TE (echo time) = 72 ms, FOV (field of view) = 2 × 2 cm^2, NEX (number of average) = 10, matrix size = 256 × 192, zero-filled at 256 × 256, corresponding to an in plane resolution of 78 × 78 μm^2. These images were used for calculation of OB volume. For morphometry, the free ImageJ software (National Institutes of Health, USA) was used. The OB area was measured in each 0.5-mm thick axial section containing the OB. Areas were expressed in mm^2 and volumes consequently calculated according to Cavalieri's principle (Roberts et al., 1993). In order to ensure consistence, one operator blind to mouse genetics performed all morphometric measurements. Further on, 1 mm-thick slices of the whole OB were acquired using a multiecho spin-echo sequence, with 10 echoes, TR of 2600 ms, and TE ranging from 20 to 200 ms, for generating quantitative T_2 mapping (Bontempi et al., 2018). T_2 maps were generated with Paravision 5.1 (Bruker, Karlsruhe, Germany).

Diffusion tensor imaging (DTI) is based on the observation of water molecule diffusivity in the brain; DTI is especially employed to characterize the orientation and integrity of the white matter (Basser et al., 2002; Le Bihan et al., 2001). DTI images were acquired with an Echo Planar Imaging (EPI) sequence optimized for the mouse olfactory bulb. Imaging parameters were set as follows: TR=3000 ms, TE=36 ms, FOV=2 × 2 cm^2, matrix size=128 × 128, 12 transversal 0.5 mm thick slices and 8 EPI segments. Diffusion images were acquired in 12 non-collinear directions with a b-value of 750 s/mm^2 (3 b0 images were acquired). DTI derived maps, Fractional Anisotropy (FA), Apparent Diffusion Coefficient (ADC), Axial Diffusivity (AD) and Radial Diffusivity (RD), were calculated with Paravison 5.1 (Bruker, Karlsruhe, Germany). Images showed no obvious distortion in the area of interest; hence a distortion correction procedure was not applied.

Comparison between the two groups of mice was carried out with the Mann-Whitney test. Results are presented as box-and-whiskers plots. Effect size (ES) was rated according to Cohen (1988) as follows: 0.2 small, 0.5 medium, 0.8 large. Correlation analysis was carried out with Spearman rho.

RESULTS

One euploid mouse died during MRI and was discarded. Age was not significantly different in the two

groups of mice (P=0.204), with euploid showing higher body mass (P=0.011; ES=1.7) as previously found (Fructuoso et al., 2017; Giacomini et al., 2018). Fig. 1 shows representative MRI images of euploid and trisomic Ts65Dn mouse head (Fig. 1A and 1E, respectively) showing the area used for OB morphometry (Fig. 1B and 1F) and T_2 maps (Fig. 1C, 1G) as well as FA (Fig. 1D, 1H). Results of MRI analysis of the olfactory bulb in trisomic and euploid Ts65Dn mice are presented in Fig. 2.

OB volume was reduced in trisomic *vs.* euploid mice, the difference being statistically significant, P=0.011, ES=1.7 (Fig. 2A). Mean absolute T_2 value appeared higher in trisomic mice as well, the difference being not significant (P=0.203 with a medium ES=0.7; Fig. 2B). All DTI variables did not differ in the two groups of mice (P>0.05, Fig. 2C-F).

Correlation analysis in the whole sample of Ts65Dn mice (n=15) showed statistically significant association between age and body mass (rho=0.74, P=0.01), while age was not correlated with OB volume (rho=0.09, P=0.742). T_2 significantly correlated in a negative way with both age (rho=-0.866, P<0.001) and body mass (rho=-0.635, P=0.011). After adjusting for body mass, the negative association between age and T_2 maps was maintained (rho=-0.862, P<0.001). No significant correlation was found between DTI variables and age or body mass.

DISCUSSION

In this work, we explored by means of MRI some structural and functional characteristics of the OB in trisomic Ts65Dn mice and compared them with euploid individuals of the same strain.

To the best of our knowledge, OB volume in DS has not been investigated in vivo. In this work, we found that OB volume is significantly lower in trisomic mice with a large ES. This is of special interest insofar overall brain size/volume is similar in trisomic and euploid Ts65Dn mice (Davisson et al., 1993; Galdzicki et al., 2001; Aldridge et al., 2007; Roubertoux et al., 2017). Intriguingly, the trisomic OB was about 87% the euploid, a reduction superimposable to that found in the cerebellum (about 88%; Baxter et al., 2000). This suggests that trisomy especially affects the OB, making this brain structure of particular interest for investigating the neurofunctional correlates of DS. In humans, OB volume is associated with olfactory function and decreases with age (Buschhutter et al., 2008). Noticeably, DS is characterized by accelerated aging and the same has been found in the Ts65Dn mouse (Vacano et al., 2012). Given the olfactory deficit in DS, it could be hypothesized that reduced OB volume in the Ts65Dn mouse is related to both accelerated aging and reduced olfactory function. This hypothesis is supported by data showing olfactory impairment in the adult Ts65Dn mouse (Guidi et al., 2017). Interestingly, reduced OB volume is also found in neurological diseases like migraine (Aktürk et al., 2019), depression (Rottstädt et al., 2018) and Parkinson's disease (Li et al., 2016), as well as in non-neurological conditions like rheumatoid arthritis (Sayilir et al., 2019) and fibromyalgia (Sayilir et al., 2017), suggesting that OB volume may be related to a variety of pathological stimuli. Further, cell cycle alteration and decreased cell proliferation has been found in brain regions different from the OB in the Ts65Dn mouse (Contestabile et al., 2007), which could contribute to reduction in OB volume. This prompts for future in vivo and ex vivo investigations linking OB volume and structural changes therein.

T_2 maps are able to provide information on the status of water in the brain (Eis et al, 1995). Longer T_2 maps values have been associated with edema (Ellingson et al., 2015), microstructural brain damage (Weissenborn et al., 2013), and myelination disorders (Lee et al., 1998; Ding et al., 2008). We herein found that mean

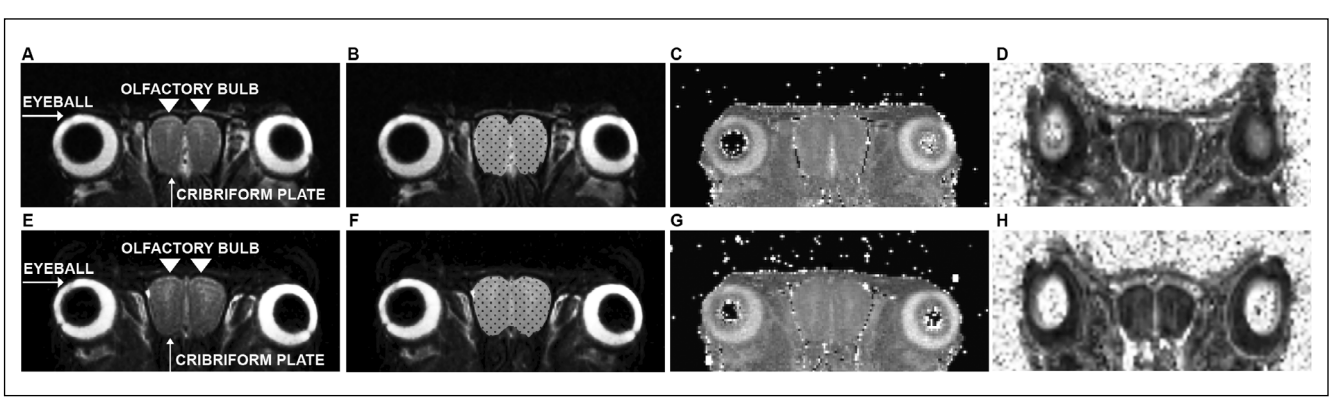

Fig. 1. Representative axial MRI pictures of Ts65Dn mouse head. A-D: euploid mouse. E-H: trisomic mouse. In panels A and E, the olfactory bulb and some other regional structures are indicated. The framed area in panels B and F was used for olfactory bulb morphometry. Panels C and G show T_2 maps. Panels D and H are fractional anisotropy images.

absolute T_2 maps value is about 8% higher in the OB of trisomic Ts65Dn mice. The difference was not statistically significant, probably due to the limited number of mice in analysis; it was, however, associated with a medium ES (0.7). ES is considered a finding of substantive significance (Cohen, 1988) and is independent of sample size. As a suggestion for future studies, we indicate that changes in the brain parenchyma may be to some extent present therein, albeit the difference in T_2 maps values of trisomic *vs.* euploid mice was

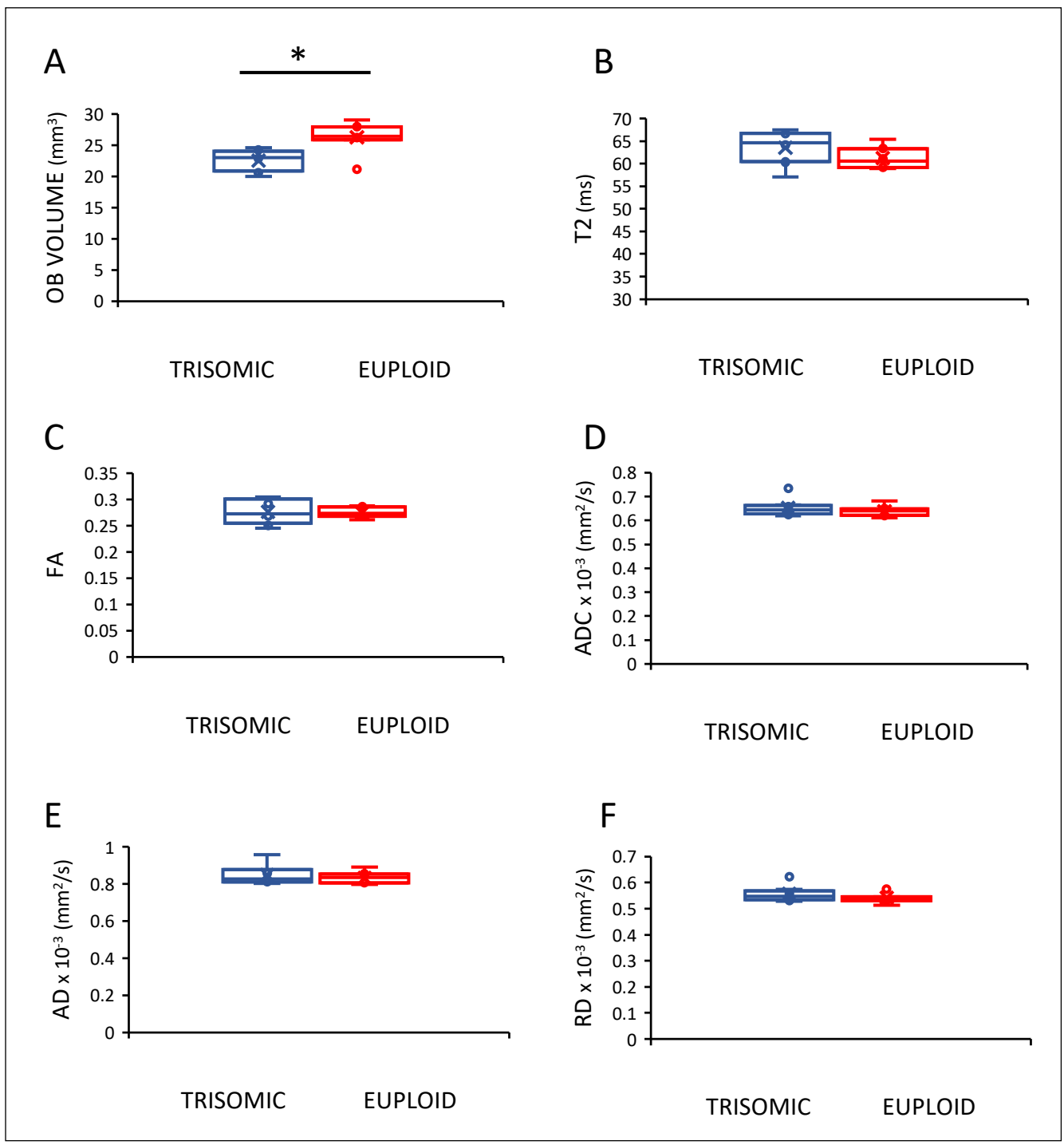

Fig. 2. Quantitative MRI variables in the olfactory bulb (OB) of trisomic Ts65Dn and euploid mice. A: OB volume is significantly smaller in trisomic mice. No difference is apparent in T_2 (B), FA (C), ADC (D), AD (E) and RD (F). FA: fractional anisotropy, ADC: apparent diffusion coefficient, AD: axial diffusivity, RD: radial diffusivity. *: P<0.05.

not statistically significant. The finding of similar DTI variables values in euploid and trisomic mice suggests that edema, instead of changes in tissue organization and/or myelin ensheathing of axons had taken place in OB. It would be expected that, in the presence of edema, consensual changes in T_2 maps value and ADC take place since ADC (also called mean diffusivity) is direction-independent, reflecting the total amount of water diffusivity in a voxel. Freedom of water diffusion and lower tissue density contribute to higher ADC (Assaf et al., 2008). Nevertheless, ADC values were similar in the two groups of mice. However, it should be underlined that T_2 maps have a better signal-to-noise ratio than DTI measurements and accordingly show increased sensitivity (Petiet et al., 2016). This may explain such a discrepancy. Further work in a larger number of mice will better characterize DTI pattern in the OB of the Ts65Dn mouse, with the aim at identifying more subtle changes therein. In fact, DTI is considered a microstructural probe operating on the micron scale (Basser et al., 2002), able to evaluate the structural integrity of nervous tissue, showing high concordance with the pathways defined in histological tracer-injection studies (Dyrby et al., 2011). In particular, fractional anisotropy (FA) is a measure of the relative diffusion along versus across fiber tracts, 0 value meaning completely isotropic diffusion and values close to 1 representing diffusion restricted to one direction (Westlin et al., 2002). FA decrease is typically dependent on the number and density of axons and is associated with neurodegenerative changes. AD is also related to axonal damage and fragmentation (Beaulieu et al., 1994). Accordingly, FA and AD are considered as markers of axonal damage. RD is related to the radial diffusivity perpendicular to white matter fascicles, hence changes in RD values are representative of axonal density and diameter, and myelination; RD is considered a marker of myelin damage.

In the whole sample of Ts65Dn mice (n=15), the finding of a negative correlation between age and T_2 of the olfactory bulb is supported by similar findings in the gray matter of normal aging brain in both humans and other species (Dhenain et al., 1997; Falangola et al., 2007; Siemonsen et al., 2008; Kumar et al., 2011; Callaghan et al., 2014). This is possibly explained by hemosiderin deposition in gray matter during the aging process.

CONCLUSIONS

Overall, the current findings show that nervous tissue alterations are detectable in vivo in the OB of the Ts65Dm mouse, an animal model of DS, which are possibly related to the olfactory deficit previously found in these mice. While results need to be confirmed in a larger number of mice and corroborated with ex-vivo morphological techniques, it is suggested that quantitative MRI is a valuable tool to identify trisomy-associated characteristics in mouse model of DS. Being non-invasive, MRI can be used for repeated measurement in the same individual, thereby allowing for longitudinal studies of the OB in DS mice.

ACKNOWLEDGEMENTS

This work was supported by local grants from University of Verona to MM and CZ, and the Italian Ministry of Research, PRIN project 2010599KBR_008 to CMC and CZ. The authors declare no conflict of interest.

REFERENCES

Aktürk T, Tanık N, Serin Hİ, Saçmacı H, İnan LE (2019) Olfactory bulb atrophy in migraine patients. Neurol Sci 40: 127–132.

Aldridge K, Reeves RH, Olson LE, Richtsmeier JT (2007) Differential effects of trisomy on brain shape and volume in related aneuploid mouse models. Am J Med Genet A 143A: 1060–1070.

Assaf Y, Pasternak O (2008) Diffusion tensor imaging (DTI)-based white matter mapping in brain research: a review. J Mol Neurosci 34: 51–61.

Basser PJ, Jones DK (2002) Diffusion-tensor MRI: theory, experimental design and data analysis - a technical review. NMR Biomed 15: 456–467.

Baxter LL, Moran TH, Richtsmeier JT, Troncoso J, Reeves RH (2000) Discovery and genetic localization of Down syndrome cerebellar phenotypes using the Ts65Dn mouse. Hum Mol Genet 9: 195–202.

Beaulieu C, Allen PS (1994) Determinants of anisotropic water diffusion in nerves. Magn Reson Med 31: 394–400.

Bianchi P, Bettini S, Guidi S, Ciani E, Trazzi S, Stagni F, Ragazzi E, Franceschini V, Bartesaghi R (2014) Age-related impairment of olfactory bulb neurogenesis in the Ts65Dn mouse model of Down syndrome. Exp Neurol 251: 1–11.

Bontempi P, Busato A, Bonafede R, Schiaffino L, Scambi I, Sbarbati A, Mariotti R, Marzola P (2018) MRI reveals therapeutical efficacy of stem cells: An experimental study on the SOD1(G93A) animal model. Magn Reson Med 79: 459–469.

Buschhüter D, Smitka M, Puschmann S, Gerber JC, Witt M, Abolmaali ND, Hummel T (2008) Correlation between olfactory bulb volume and olfactory function. Neuroimage 42: 498–502.

Callaghan MF, Freund P, Draganski B, Anderson E, Cappelletti M, Chowdhury R, Diedrichsen J, Fitzgerald TH, Smittenaar P, Helms G, Lutti A, Weiskopf N (2014) Widespread age-related differences in the human brain microstructure revealed by quantitative magnetic resonance imaging. Neurobiol Aging 35: 1862–1872.

Cecchini MP, Viviani D, Sandri M, Hähner A, Hummel T, Zancanaro C (2016) Olfaction in people with down syndrome: a comprehensive assessment across four decades of age. PLoS One 11: e0146486.

Cohen J (1988) Statistical Power Analysis for the Behavioral Sciences 2nd ed. Lawrence Erlbaum Associates, Hillsdale (NJ).

Contestabile A, Fila T, Ceccarelli C, Bonasoni P, Bonapace L, Santini D, Bartesaghi R, Ciani E (2007) Cell cycle alteration and decreased cell proliferation in the hippocampal dentate gyrus and in the neocortical

germinal matrix of fetuses with Down syndrome and in Ts65Dn mice. Hippocampus 17: 665–678.

Davisson MT, Schmidt C, Reeves RH, Irving NG, Akeson EC, Harris BS, Bronson RT (1993) Segmental trisomy as a mouse model for Down syndrome. Prog Clin Biol Res 384: 117–133.

Dhenain M, Duyckaerts C, Michot JL, Volk A, Picq JL, Boller F (1998) Cerebral T2-weighted signal decrease during aging in the mouse lemur primate reflects iron accumulation. Neurobiol Aging 19: 65–69.

Ding XQ, Wittkugel O, Goebell E, Förster AF, Grzyska U, Zeumer H, Fiehler J (2008) Clinical applications of quantitative T2 determination: a complementary MRI tool for routine diagnosis of suspected myelination disorders. Eur J Paediatr Neurol 12: 298–308.

Dyrby TB, Baare WF, Alexander DC, Jelsing J, Garde E, Sogaard LV (2011) An *ex vivo* imaging pipeline for producing high-quality and high-resolution diffusion-weighted imaging datasets. Hum Brain Mapp 32: 544–563.

Eis M, Els T, Hoehn-Berlage M (1995) High resolution quantitative relaxation and diffusion MRI of three different experimental brain tumors in rat. Magn Reson Med 34: 835–844.

Ellingson BM, Lai A, Nguyen HN, Nghiemphu PL, Pope WB, Cloughesy TF (2015) Quantification of nonenhancing tumor burden in gliomas using effective T2 maps derived from Dual-Echo Turbo Spin-Echo MRI. Clin Cancer Res 21: 4373–4383.

Falangola MF, Dyakin VV, Lee SP, Bogart A, Babb JS, Duff K, Nixon R, Helpern JA (2007) Quantitative MRI reveals aging-associated T2 changes in mouse models of Alzheimer's disease. NMR Biomed 20: 343–351.

Fructuoso M, Rachdi L, Philippe E, Denis RG, Magnan C, Le Stunff H, Janel N, Dierssen M (2018) Increased levels of inflammatory plasma markers and obesity risk in a mouse model of Down syndrome. Free Radic Biol Med 114: 122–130.

Galdzicki Z, Siarey R, Pearce R, Stoll J, Rapoport SI (2001) On the cause of mental retardation in Down syndrome: extrapolation from full and segmental trisomy 16 mouse models. Brain Res Brain Res Rev 35: 115–145.

Giacomini A, Stagni F, Emili M, Guidi S, Salvalai ME, Grilli M, Vidal-Sanchez V, Martinez-Cué C, Bartesaghi R (2018) Treatment with corn oil improves neurogenesis and cognitive performance in the Ts65Dn mouse model of Down syndrome. Brain Res Bull 140: 378–391.

Guidi S, Bianchi P, Stagni F, Giacomini A, Emili M, Trazzi S, Ciani E, Bartesaghi R (2017) Lithium restores age-related olfactory impairment in the Ts65Dn mouse model of Down syndrome. CNS Neurol Disord Drug Targets 16: 812–819.

Korenberg JR, Chen XN, Schipper R, Sun Z, Gonsky R, Gerwehr S, Carpenter N, Daumer C, Dignan P, Disteche C (1994) Down syndrome phenotypes: the consequences of chromosomal imbalance. Proc Natl Acad Sci USA 91: 4997–5001.

Kumar R, Delshad S, Woo MA, Macey PM, Harper RM (2012) Age-related regional brain T2-relaxation changes in healthy adults. J Magn Reson Imaging 35: 300–308.

Le Bihan D, Mangin JF, Poupon C, Clark CA, Pappata S, Molko N, Chabriat H (2001) Diffusion tensor imaging: concepts and applications. J Magn Reson Imaging 13: 534–546.

Lee MA, Smith S, Palace J, Matthews PM (1998) Defining multiple sclerosis disease activity using MRI T2-weighted difference imaging. Brain 121: 2095–2102.

Li J, Gu CZ, Su JB, Zhu LH, Zhou Y, Huang HY, Liu CF (2016) Changes in olfactory bulb volume in Parkinson's disease: a systematic review and meta-analysis. PLoS One 11: e0149286.

López-Hidalgo R, Ballestín R, Vega J, Blasco-Ibáñez JM, Crespo C, Gilabert-Juan J, Nácher J, Varea E (2016) Hypocellularity in the murine model for Down syndrome Ts65Dn is not affected by adult neurogenesis. Front Neurosci 10: 75.

Mann DM, Yates PO, Marcyniuk B, Ravindra CR (1986) The topography of plaques and tangles in Down's syndrome patients of different ages. Neuropathol Appl Neurobiol 12: 447–457.

Mori K, Nagao H, Yoshihara Y (1999) The olfactory bulb: coding and processing of odor molecule information. Science 286: 711–715.

Murphy C, Jinich S (1996) Olfactory dysfunction in Down's syndrome. Neurobiol Aging 17: 631–637.

Neale N, Padilla C, Fonseca LM, Holland T, Zaman S (2017) Neuroimaging and other modalities to assess Alzheimer's disease in Down syndrome. Neuroimage Clin 17: 263–271.

Parker SE, Mai CT, Canfield MA, Rickard R, Wang Y, Meyer RE, Anderson P, Mason CA, Collins JS, Kirby RS, Correa A; National Birth Defects Prevention Network (2010) Updated National Birth Prevalence estimates for selected birth defects in the United States, 2004–2006. Birth Defects Res A Clin Mol Teratol 88: 1008–1016.

Petiet A, Aigrot MS, Stankoff B (2016) Gray and white matter demyelination and remyelination detected with multimodal quantitative MRI analysis at 11.7T in a chronic mouse model of multiple sclerosis. Front Neurosci 10: 491.

Price JL, Davis PB, Morris JC, White DL (1991) The distribution of plaques, tangles, and related immunohistochemical markers in healthy aging and Alzheimer's disease. Neurobiol Aging 12: 295–312.

Roubertoux PL, Baril N, Cau P, Scajola C, Ghata A, Bartoli C, Bourgeois P, di Christofaro J, Tordjman S, Carlier M (2017) Differential brain, cognitive and motor profiles associated with partial trisomy. Modeling Down syndrome in mice. Behav Genet 47: 305–322. [correction in Behav Genet. 47: 323.

Roberts N, Cruz-Orive LM, Reid NM, Brodie DA, Bourne M, Edwards RH (1993) Unbiased estimation of human body composition by the Cavalieri method using magnetic resonance imaging. J Microsc 171: 239–253.

Rottstädt F, Han P, Weidner K, Schellong J, Wolff-Stephan S, Strauß T, Kitzler H, Hummel T, Croy I (2018) Reduced olfactory bulb volume in depression - A structural moderator analysis. Hum Brain Mapp 39: 2573–2582.

Sayılır S, Çullu N (2017) Decreased olfactory bulb volumes in patients with fibromyalgia syndrome. Clin Rheumatol 36: 2821–2824.

Sayılır S, Çullu N, Mengi G, Ekiz T (2019) Evaluation of olfactory bulb volumes in patients with rheumatoid arthritis: A retrospective study. Arch Rheumatol 34: 334–337.

Siemonsen S, Finsterbusch J, Matschke J, Lorenzen A, Ding XQ, Fiehler J (2008) Age-dependent normal values of T2* and T2' in brain parenchyma. AJNR Am J Neuroradiol 29: 950–955.

Vacano GN, Duval N, Patterson D (2012) The Use of mouse models for understanding the biology of Down syndrome and aging. Curr Gerontol Geriatr Res 2012: 717315.

Weissenborn K, Bültmann E, Donnerstag F, Giesemann AM, Götz F, Worthmann H, Heeren M, Kielstein J, Schwarz A, Lanfermann H, Ding XQ (2013) Quantitative MRI shows cerebral microstructural damage in hemolytic-uremic syndrome patients with severe neurological symptoms but no changes in conventional MRI. Neuroradiology 55: 819–825.

Westin CF, Maier SE, Mamata H, Nabavi A, Jolesz FA, Kikinis R (2002) Processing and visualization for diffusion tensor MR imaging. Med Image Anal 6: 93–108.

William CM, Saqran L, Stern MA, Chiang CL, Herrick SP, Rangwala A, Albers MW, Frosch MP, Hyman BT (2017) Activity-dependent dysfunction in visual and olfactory sensory systems in mouse models of Down syndrome. J Neurosci 37: 9880–9888.